The 20th International Symposium on Transport Phenomena
7-10 July, 2009, Victoria BC, CANADA
SAND2009-2058C

HEAT AND MASS TRANSPORT DURING EROSION OF SOLID SUBSTRATE BY PROPELLANT FIRE

Fan-Bill Cheung[1*], *Sang-Ki Moon*[1**], *John Hewson*[2] *and William Erikson*[2]

[1] Pennsylvania State University, University Park, PA, USA
[2] Sandia National Laboratories, Albuquerque, NM, USA

ABSTRACT

The interaction between liquid aluminum and solid substrates during an accidental solid-propellant fire is studied to seek a better understanding of the relevant heat and mass transport processes and the underlying physics and to predict the rates of erosion. A scaling analysis is made to estimate the magnitudes of the dimensionless parameters that control the flow behavior based upon which criteria for the occurrence of various erosion regimes are determined. Extension of previous models is then performed to obtain suitable correlation equations for predicting the rates of erosion under different flow and temperature conditions. It is found that the initial temperatures of the molten substance and the solid substrates have important impact on the erosion behavior of the system. For dissolution mass transport, the primary parameters controlling the rate of erosion are the mass diffusivity and the solubility. In general, a higher erosion rate is obtained as either the mass diffusivity or the solubility is increased. For impingement melting heat transport, the primary parameters controlling the rate of erosion are the Stefan number, the jet Reynolds number, and the Prandtl number. In general, the rate of erosion is highest for the turbulent-flow melting regime without crust formation and lowest for the turbulent-flow melting regime with crust formation. The latter could be an order of magnitude lower than the rate of erosion for the laminar-flow melting regime.

I. INTRODUCTION

The interaction between liquid aluminum and solid substrate including steel, carbon, and iridium taking place in an accidental solid-propellant fire is an important safety concern in space vehicle launches. Aluminum particles are often included in the formulation of solid propellants to improve performance. The aluminum particles burn more gradually than the primary components of the solid propellant. During a propellant-fire accident resulting from, for example, the breakup of solid-propellant rocket motors, it is possible for burning aluminum particles in the form of agglomerated liquid droplets that are dispersed in the high-temperature plume of the primary propellant to travel some distance and deposit on the surfaces of nearby substrates. Usually the number density of the aluminum droplets is high enough to form a molten aluminum layer (with alumina solid particles in it) on the substrate surface. Upon formation of the molten layer, erosion of the substrate material would occur as a result of dissolution or melting. Metal dissolution/erosion/melting in conjunction with deposits of molten aluminum and aluminum oxide in propellant fire environments has been observed experimentally in the past (Hunter et al. 2007). However, the relevant processes occurring between the deposit and the substrate material are not fully understood.

Depending on the time duration and the fire environment, erosion of a solid substrate could take place either by melting, dissolution mass transport, corrosion, mechanical scouring, or chemical reactions. However, over the ranges of temperature and flow conditions anticipated in a solid-propellant fire, only melting and dissolution mass transport are of important concern. The subject of impingement melting, wherein melting of a solid substrate by a molten impinging jet takes place under forced-thermal-convection conditions, has been studied quite extensively in the past, as summarized in the review article by Martin (1977). Epstein et al. (1980) considered the process of simultaneous melting and freezing in the impingement region of a liquid jet and presented a correlation equation for impingement melting heat transfer under laminar flow conditions. Saito et al. (1990, 1991) conducted a theoretical and experimental study on impingement melting heat transfer under turbulent flow conditions with or without crust formation at the interface between the impinging jet and the solid wall. They found substantial reduction in the impingement melting heat transfer due to the presence of crust, which presumably inhibits forced convection.

In the scenarios under consideration in this study, dissimilar molten and substrate materials are of interest. In such environments, the substrate can dissolve into a molten deposit to the extent permitted by chemical activities. The subject of dissolution mass transport has been studied extensively by previous investigators. Gairola et al. (1971) measured the dissolution of a vertical nickel cylinder in molten aluminum whereas Niinomi et al. (1982) investigated the dissolution of ferrous alloys in molten aluminum. Both studies were made under free convection conditions. In a later study, Niinomi et al. (1984) also investigated the dissolution of ferrous alloys in molten aluminum under forced convection conditions. Dybkov (1990) studied the dissolution of steel in molten aluminum and found the process to be non-selective with the solubility of steel being essentially the same as the solubility of iron in aluminum. While these experimental works provide some useful data on the material composition and the overall dissolution, they offer very little information on the characteristic features of the dissolution heat and mass transport processes. In an attempt to seek a better understanding of the underlying physical mechanisms, Shiah et al. (1998) investigated the process of dissolution mass transport for an isothermal binary metallic system under natural convection conditions. They obtained a correlation equation for the Sherwood number as a function of the saturated concentration at the interface between the solid substrate and the molten substance. Boral and Cheung (2000)

[*] Corresponding author: fxc4@psu.edu
[**] Currently with the Korea Atomic Energy Research Institute

extended the work of Shiah et al. (1998) to the general case of a non-isothermal system taking full account of the density variations with concentration and temperature. Later, Boral et al. (2002) presented correlations equations for dissolution heat and mass transport in an aluminum-steel system. These analyses demonstrated that the dissolution-rate-limiting process under these conditions is the mass transport of the dissolved substance. All of these theoretical studies, however, were limited to the case of natural convection flow.

In the present study, an attempt is made to seek a better understanding of the relevant processes involved in the erosion of a solid substrate upon impingement by a molten aluminum jet resulting from a solid-propellant fire. The ultimate goal is to determine the erosion rate under various flow and temperature conditions. Specific objectives are: (i) to identify the dominant processes taking place between the molten layer and the substrate, (ii) to extend the models developed by previous investigators to account for the underlying physics of the dominant processes, and (iii) to predict the rates of erosion for different erosion regimes under different flow and temperature conditions.

II. THERMOPHYSICAL PROPERTIES OF MOLTEN ALUMINUM AND SUBSTRATES

To meet the above objectives, it is necessary to first determine the thermophysical properties of the aluminum-substrate systems as functions of temperature. The substrate materials of interest include iron (Fe), pyrolytic graphite (C), and iridium (Ir). This requires consideration of four molten mixtures including pure Al, Al-Fe, Al-C, and Al-Ir. The temperatures to be explored for the solid phase ranges from 300 K to 1100 K, for molten aluminum from 1500 K to 2700 K, and for molten mixtures from the contact temperature at the solid-liquid interface to the ambient temperature of molten aluminum.

Saturated Concentration (Solubility)

The saturated concentrations, C_s, of iron and iridium in liquid aluminum are found from the phase diagrams (Predel, 1991). The following solubility correlation for the carbon in liquid aluminum can be obtained using experimental data of Oden (1989):

$$\ln C_s = 12.231 - 24322.96/T \tag{1}$$

where C_s is in wt %, T is the temperature in degrees Kelvin, respectively.

Mass Diffusion Coefficient (or Mass Diffusivity)

Owing to the absence of experimental data, the diffusion coefficients of substrates into molten aluminum are estimated using a simple Stokes-Einstein formula (Iida and Guthrie, 1988):

$$D = k_B T/(6\pi\mu r) \tag{2}$$

where D is in m^2/s, k_B the Boltzmann's constant, μ the dynamic viscosity of the melt in Pa-s, and r the atomic radius in the melt in m. The diffusion coefficient obtained from the Stokes-Einstein formula represents an upper limit as the chemical interaction in the melts is not accounted for as indicated by Khina et al. (2005). Guminski (1995) reported that the Stokes-Einstein formula shows reasonable predictions for the diffusion coefficient for various metals and non-metals in various liquid metals.

Surface Tension

The surface tension can drive flow in the presence of temperature or composition gradients. To determine whether this effect is significant or not, the magnitude of the surface tension, σ, and its temperature gradient, $d\sigma/dT$, need to be estimated. This is done using experimental data of Nizhenko and Floka (1972) as shown in Table 1.

Table 1. Information on the Surface Tension of Pure Liquid Metals

Parameter	Al	Fe	Ir
Atomic mass, M_i (g/mol)	26.981	55.845	192.217
ρ_0 (kg/m^3)	2385	7015	19500
$d\rho/dT$ (kg/m^3-K)	-0.280	-0.883	-0.850
σ_0 (10^{-3} N/m)	914	1872	2230
$d\sigma_0/dT$ (10^{-3} N/m-K)	-0.35	-0.49	-0.17
T_0 (K)	933.15	1809.15	2719.00

III. CONTACT TEMPERATURE

To realistically predict the rates of erosion over different temperature ranges and flow conditions, it is necessary to first identify the prevailing erosion regimes. For the case in which the contact temperature at the interface between the solid substrate and the molten layer is above the melting point of the substrate, direct melting of the solid substrate would take place. The rate of erosion can readily be estimated from the published results on impingement melting heat transfer (Epstein et al. 1980; Saito et al. 1990, 1991).

When two semi-infinite bodies at different initial temperatures are suddenly brought into contact, each body will instantaneously come to some intermediate contact temperature at its interface. Since the region affected by the contact is very small compared to the physical dimensions of the two bodies, most substances can be treated as semi-infinite during the initial period of contact. This applies also to the substrate-molten aluminum systems under consideration. According to Myers (1971), the contact temperature at the interface between the substrate (i.e., the wall) and the molten aluminum upon sudden contact can be determined from the following equation

$$T_c = (T_{fi} + bT_{wi})/(1+b) \tag{3}$$

where T_{wi} is the initial temperature of the wall, T_{fi} the initial temperature of the molten aluminum, and b the thermal property ratio of the wall and the molten aluminum defined by

$$b = \sqrt{(k\rho c_p)_w/(k\rho c_p)_f} \tag{4}$$

In the above equation, k is the thermal conductivity, ρ the density, c_p the specific heat; the subscript "w" refers to the wall whereas the subscript "f" refers to the molten aluminum.

Note that the semi-infinite assumption may no longer be valid during a long exposure as the contact temperature will change from what it is initially. There is also the issue of continued heating by thermal radiation that will affect the temperature at the substrate-deposit interface. In addition, if solidification of the molten aluminum and/or melting of the solid substrate would occur upon contact, then the contact temperature would have to be determined differently as described by Epstein (1973). In this study, the semi-infinite assumption is employed as a first approximation.

It was found that, over the anticipated ranges of the initial temperatures of the wall and the molten aluminum, the contact temperature is always below the melting point of the wall when the substrate material is either iridium or graphite. When the substrate material is iron, melting of the wall could occur only at high initial temperatures. Should the initial wall temperature be below ~ 800 K or the initial molten aluminum below 2400 K, no wall melting would occur.

IV. SCALING ANALYSIS

When the contact temperature is below the melting point of the substrate, erosion can take place only by dissolution mass transport or other chemical reaction processes. The chemical processes are typically fast relative to mass transport in the liquid phase so that the resulting erosion rate depends primarily on the prevailing flow regimes involved in the dissolution mass transport processes. In this section, a scaling analysis of the relevant processes is performed under dissolution mass transport conditions by considering the magnitudes of the dimensionless parameters that describe the relative importance of the driving forces for the flow. These parameters include the Grashof number, the Reynolds number, the Marangoni number, and the Bond number. The goal is to identify the dominant mass transport processes under various conditions.

The dimensionless parameter describing the relative importance of the buoyancy force and the viscous force under natural convection flow is the Grashof number. Accounting for the buoyancy induced by both the concentration gradients and the temperature gradients (Boral et al. 2002), the Grashof number, Gr_L, is given by

$$Gr_L = \frac{g(\Delta\rho/\rho_s)L^3}{v_s^2} = \frac{g\left((1-d)C_s + \overline{\beta}\Delta T\right)L^3}{v_s^2} \qquad (5)$$

where g is the acceleration due to gravity, $\Delta\rho$ the density difference across the molten layer, ρ_s the mixture density at the interface between the solid substrate and the molten layer, L the characteristic length of the solid substrate, d the density ratio between the molten substance and the solid substrate, i.e., $d = \rho_f/\rho_w$, C_s the saturated concentration at the interface, $\overline{\beta}$ the thermal expansion coefficient of the molten substance, ΔT the temperature difference across the molten layer, i.e., $\Delta T = T_f - T_c$, and v_s the viscosity of the molten substance at the interface. Assuming a linear dependence on the saturated concentration, the thermal expansion coefficient of the molten substance can be evaluated as $\overline{\beta} = C_s\beta_w + (1-C_s)\beta_f$, where β_w is the thermal expansion coefficient of the substrate and β_f the thermal expansion coefficient of the molten aluminum. In the above expressions, the density and the kinematic viscosity of the molten substance at the interface are defined respectively by

$$\rho_s = \rho_{m,s}\left[1-\left(1-\frac{\rho_{m,s}}{\rho_{w,s}}\right)C_s\right]^{-1} \text{ and } v_s = \mu_s/\rho_s \qquad (6)$$

For forced convection flow, the inertial force is attributed here to a molten jet impinging on the substrate surface in a stagnation flow pattern. The dimensionless parameter describing the relative importance of the inertial force and the viscous force under forced convection flow is the Reynolds number, Re_d, given by

$$Re_d = \rho_{m,s}u_\infty d_e/\mu_s \qquad (7)$$

where $\rho_{m,s}$ is the density of the molten substance at the interface between the solid substrate and the molten layer, u_∞ the freestream velocity of the molten layer caused by the shear action of the impinging jet, d_e the diameter of the impinging jet, and μ_S the absolute viscosity of the molten substance.

The dimensionless parameter describing the relative importance of the thermocapillary force and the viscous force under Marangoni flow is the Marangoni number, Ma_L, given by

$$Ma_L = \left|\frac{d\sigma}{dT}\right|\frac{\delta\Delta T}{\alpha v_s} \qquad (8)$$

where σ is the surface tension, T the absolute temperature of the molten substance, δ the thickness of the molten layer, and α the thermal diffusivity of the molten substance.

The above dimensionless parameters are compared to investigate the relative importance of the various dissolution mass transfer processes. The relative importance of the natural convection and the forced convection flow is measured by the following dimensionless ratio R:

$$R = Gr_L/Re_d^2 \qquad (9)$$

On the other hand, the relative importance of the natural convection and Marangoni convection flow is measured by the Bond number defined by:

$$Bo^* = Gr_L Pr/Ma_L = \frac{g\Delta\rho L^3}{\left|d\sigma/dT\right|\delta\Delta T} \qquad (10)$$

where the density difference is given by

$$\Delta\rho = \rho_s\left[(1-d)C_s + \overline{\beta}\Delta T\right] \qquad (11)$$

Results on the relative importance of the various dissolution mass transfer-dominated regimes are shown in Figs. 1 and 2. As can be seen from Fig. 1, natural convection could be more or less important than forced convection, depending on the characteristic length of the substrate. In general, both need to be accounted for in assessing the erosion rates under dissolution mass transport conditions. Note that for a given characteristic length, the effect of natural convection is more pronounced for the Al-Fe system than the Al-Ir system. The effect of natural convection for the latter system is in turn more pronounced than the Al-C system.

The relative importance of natural convection and Marangoni convection is presented in Fig. 2 for the Al-Fe system. (Similar results have been obtained for the Al-Ir and Al-C systems but are not presented due to space limitation.) For all three systems, the Bond number is several orders of magnitude larger than unity, indicating that the effect of Marangoni convection is negligible compared to the effect of natural convection. As such, there is no need to account for the effect of Marangoni convection in assessing the erosion rates under dissolution mass transport conditions.

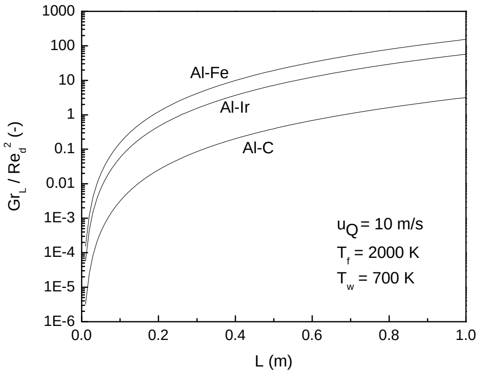

Figure 1. Effect of the Characteristic Length on Forced and Natural Convection

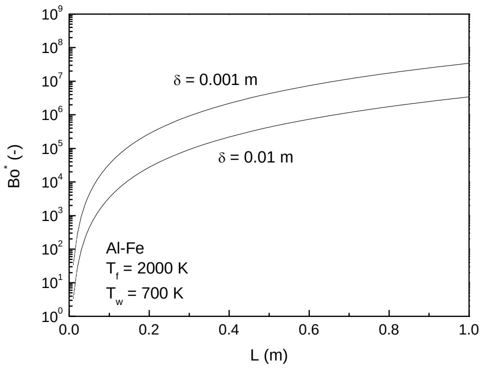

Figure 2. Effect of the Characteristic Length on the Bond Number

V. NUMERICAL PREDICTION OF THE RATES OF EROSION

Based on the results of scaling analysis, various regimes can be identified. In each of the relevant regimes, numerical simulations of the variable-density Navier-Stokes equations have been carried out (in some cases taking advantage of previous work) to determine the erosion rates. The later is expressed in terms of a surface regression velocity defined by

$$v_0 = -\frac{D}{1-C_s}\left.\frac{\partial C}{\partial y}\right|_{y=0} \tag{12}$$

where the concentration gradient is evaluated at the substrate surface, y = 0.

Natural Convection Dissolution Regime

When the dissolution process is primarily due to natural convection with negligible effects of forced convection, correlation equations for the dissolution mass transport have been obtained by Boral et al. (2002). By extending their correlations to the case for which the natural convection flow is induced primarily by the concentration gradients across the concentration boundary layer, the following expression can be derived for the rate of erosion, v_0:

$$v_0 = 0.64\frac{D}{L}\left[1+0.27C_s+0.12C_s^2\right]C_s Sc^{1/4} Gr_{c,L}^{1/4} \tag{13}$$

where Sc and $Gr_{c,L}$ are the Schmidt number and the average species Grashof number, respectively. The latter two quantities are defined by:

$$Sc = \frac{\nu_s}{D} = \frac{\mu_s}{\rho_s D} \tag{14}$$

$$Gr_{c,L} = \frac{g\left|(1-d)C_s\right|L^3}{\nu_s^2} \tag{15}$$

Similarly, by extending the correlation of Boral et al. (2002) to the case for which the natural convection flow is induced primarily by the temperature gradients across the thermal boundary layer, the following expression can be derived for the rate of erosion:

$$v_0 = 0.83\frac{D}{L}\left[1+0.27C_s+0.47C_s^2\right]C_s Sc^{1/3} Gr_{t,L}^{1/4} \tag{16}$$

where $Gr_{t,L}$ is an average Grashof number across the thermal boundary layer given by:

$$Gr_{t,L} = g\bar{\beta}\Delta T L^3 / \nu_s^2 \tag{17}$$

Using the thermophysical properties presented in section II for the Al-Fe, Al-Ir, and Al-C systems, the rates of erosion can be calculated from the above equations for different values of the characteristic length of the substrate and the initial temperatures of the solid and molten phases. Numerical results for the three systems under consideration for flows induced primarily by the concentration gradients are shown in Figs. 3 and 4. Similar results are obtained for flows induced by the temperature gradients.

Figure 3 presents the variation of the erosion rate with the characteristic length of the substrate, with the initial temperatures of the wall and the molten aluminum being fixed at 700 K and 2000 K, respectively. As can be seen from the figure, for all three systems, the erosion rate tends to decrease as the substrate length is increased. However, there are significant differences in the erosion rate among the three systems. Whereas the rate of erosion of iron is almost an order of magnitude higher than the corresponding rate of erosion of iridium, the rate of erosion of graphite is nearly two orders of magnitude lower than the corresponding rate of erosion of iridium.

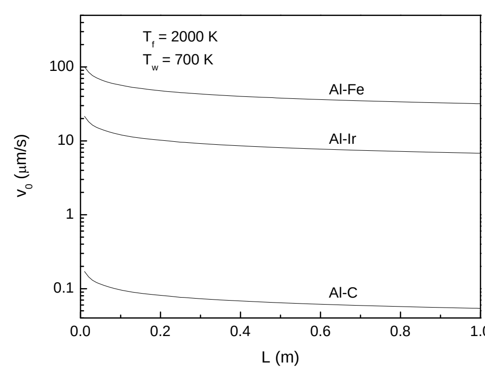

Figure 3. Length Effect on Concentration-controlled Natural Convection Erosion

Figure 4 presents the variations of the erosion rate with the initial temperatures of the wall and the molten aluminum for the Al-Fe system. (Similar results have been obtained for the Al-Ir and Al-C systems but are not presented due to space limitation.) For all three systems under consideration, the erosion rate is a strong function of the initial temperatures. A higher erosion rate is obtained as either the initial wall temperature or the initial temperature of the molten aluminum is increased. On the other hand, over the entire ranges of initial temperatures explored in this study, the erosion rate is found to decrease as the substrate length is increased. For all initial temperatures and substrate lengths considered in this study, the rate of erosion of iron is at least several times higher than the corresponding rate of erosion of iridium whereas the rate of erosion of graphite is at least an order of magnitude lower than the corresponding rate of erosion of iridium.

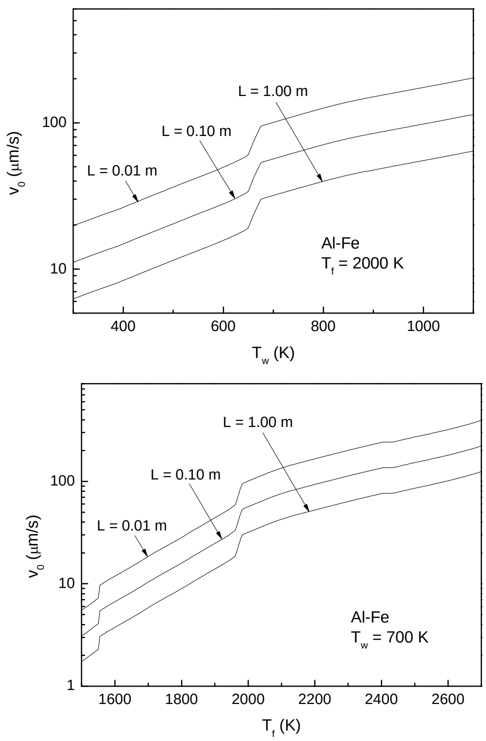

Figure 4. Concentration-controlled Erosion Regime for the Al-Fe System

Forced Convection Dissolution Regime

For heat and mass transport by an impinging jet upon a flat plate without the occurrence of melting, correlation equations have been presented by Martin (1977) for the Sherwood and Nusselt numbers. By extending Martin's correlations to the present case, the following expression can be derived for the rate of erosion, v_0:

$$v_0 = 0.53\frac{D}{d_e}\left[1+0.27C_s\right]C_s Sc^{0.42} Re_d^{0.5}\left[1+\frac{Re_d^{0.55}}{200}\right]^{1/2} \qquad (18)$$

where Re_d is the Reynolds number given by

$$\mathrm{Re}_d = u_\infty d_e / \nu_s \qquad (19)$$

where u_∞ is the ambient velocity of the molten layer induced by the shear action of the impinging jet. Note that the molten aluminum particles are travelling at a slower speed than the gas plume from the solid-propellant fire. As such, the value of u_∞ is taken to be much lower than the velocity of the two-phase plume.

Figure 5 presents the variation of the erosion rate with the ambient velocity, with the initial temperatures of the wall and the molten aluminum being fixed at 700 K and 2000 K, respectively. As can be seen from the figure, for all three systems, the erosion rate tends to increase as the ambient velocity is increased. However, there are appreciable differences in the erosion rate among the three systems. Whereas the rate of erosion of iron is several times higher than the corresponding rate of erosion of iridium, the rate of erosion of graphite is always an order of magnitude lower than the corresponding rate of erosion of iridium.

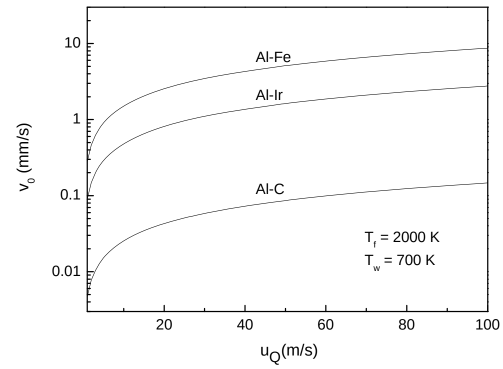

Figure 5. Effect of Jet Velocity on Forced Convection Erosion

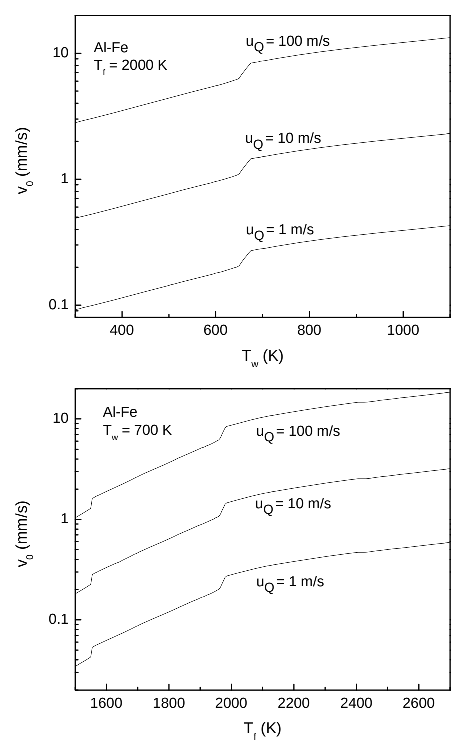

Figure 6. Effect of the Initial Temperatures on Forced Convection Erosion

Figure 6 presents the variations of the erosion rate with the initial temperatures of the wall and the molten aluminum for the Al-Fe system. (Similar results have been obtained for the Al-Ir and Al-C systems but are not presented due to space limitation.) For all three systems under consideration, the erosion rate is a strong function of the initial temperatures. A higher erosion rate is obtained as either the initial wall temperature or the initial temperature of the molten aluminum is increased. This behavior is similar to those observed under natural convection conditions shown in Figs. 3 and 4. On the other hand, over the entire ranges of initial temperatures explored in this study, the erosion rate is found to increase substantially as the ambient velocity is increased. For all initial temperatures and ambient velocities considered in this study, the rate of erosion of iron is always several times higher than the corresponding rate of erosion of iridium whereas the rate of erosion of graphite is nearly an order of magnitude lower than the corresponding rate of erosion of iridium. Again, this behavior is similar to those observed under natural convection conditions shown in Figs. 3 and 4.

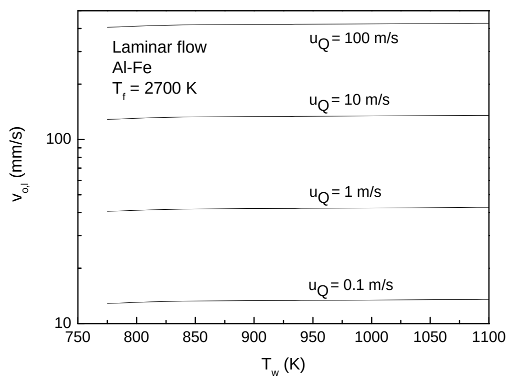

(a) Laminar-Flow Melting Regime

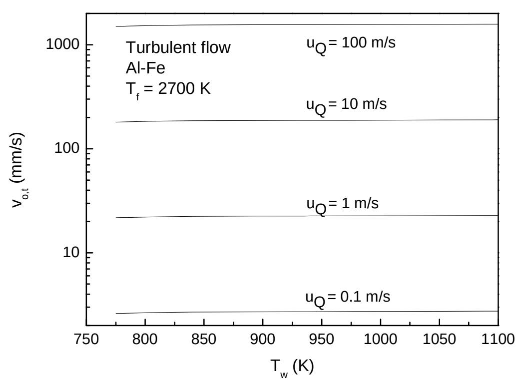

(b) Turbulent-Flow Melting Regime

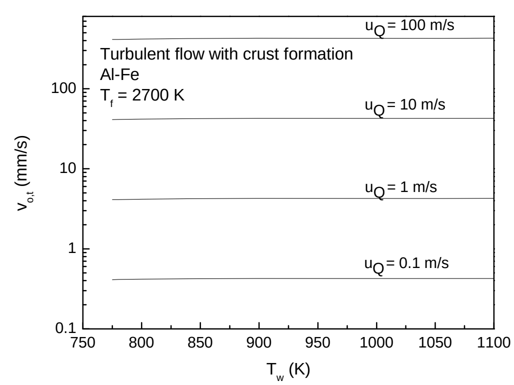

(c) Turbulent-Flow Melting Regime with Crust Formation
Figure 7. Melting-Controlled Erosion Rates

Melting-Controlled Erosion Regime

When melting of the substrate occurs, the rate of erosion would depend primarily on heat transport rather than mass transport. Depending upon whether the impinging flow is laminar or turbulent and whether or not there is crust formation at the interface between the solid substrate and the impinging liquid jet, considerably different rates of erosion could be anticipated.

Under laminar flow conditions, a correlation equation for impingement melting heat transfer has been obtained by Epstein et al. (1980), based upon which the following expression for the laminar-flow melting regime can be derived for the rate of erosion, v_0:

$$v_{o,l} = \frac{k(T_\infty - T_{w,mp})}{d_e \rho_w \Delta H_f} 0.55\sqrt{2} Re_d^{0.5} Pr^{0.35} \qquad (20)$$

On the other hand, under turbulent flow conditions, a correlation equation for impingement melting heat transfer without crust formation has been obtained by Saito et al. (1991), based upon which the following expression for the turbulent-flow melting regime can be derived for the rate of erosion, v_0:

$$v_{o,t} = \frac{k(T_\infty - T_{w,mp})}{d_e \rho_w \Delta H_f} 0.0152 Re_d^{0.92} Pr^{0.8} \qquad (21)$$

When there is crust formation at the interface between the molten jet and the wall, Saito et al. (1990) observed appreciably lower rates of impingement melting heat transfer under turbulent flow conditions. Based upon their correlation, the following expression for the turbulent-flow melting regime with crust formation can be derived for the rate of erosion, v_0:

$$v_{o,t} = \frac{k(T_\infty - T_{w,mp})}{d_e \rho_w \Delta H_f} 0.0033 Re_d Pr \qquad (22)$$

In the above equations, T_∞ is the temperature of molten aluminum at infinity, $T_{w,mp}$ the melting temperature of the substrate, k the thermal conductivity of the substrate, ΔH_f the latent heat of fusion of the substrate at the melting temperature, and Re_d is the Reynolds number given by equation (7), and Pr the Prandtl number of the molten jet. The jet diameter, d_e, is taken to be 0.0254 m. Again, the value of u_∞ in the above equation is taken to be much lower than the velocity of the two-phase plume from the solid-propellant fire as the molten aluminum particles are travelling at a slower speed.

Note from equations (20) to (22) that the rates of erosion for both laminar and turbulent flows with or without crust formation are always dependent upon the ratio of the sensible heat and the latent heat. This ratio is the so-called Stefan number, St, given by

$$St = C_p(T_\infty - T_{w,mp}) / \Delta H_f \qquad (23)$$

Note that impingement melting of the wall is expected to occur only in the Al-Fe system. For Al-Ir and Al-C systems, the contact temperatures (see Section III) are always below the melting point of the substrates (i.e., Ir and C) and as such, no melting-controlled erosion would take place in these two systems.

Numerical results for the three different flow regimes (i.e., laminar-flow melting regime, turbulent-flow melting regime without crust formation, and turbulent-flow melting regime with crust formation) are shown in Fig. 7 whereas the effects of jet velocity and Reynolds number are shown in Fig. 8.

Figure 7 presents the variations of the erosion rate with the initial temperature of the wall for the three different regimes. The ambient velocity is treated as a parameter. For all three regimes, the erosion rate is a weak function of the initial temperatures of the substrate and the molten jet (as long as the contact temperature is above the melting point of the substrate). On the contrary, the erosion rate is a strong function of the jet velocity in all three regimes. As the jet velocity is increased, the erosion rate tends to increase considerably. Note that the erosion rate for the turbulent-flow melting regime in the absence of crust formation is much higher than the erosion rate for the laminar-flow melting regime. If, however, there is crust formation, the rate of erosion in the turbulent-flow regime could be well below the erosion rate for laminar-flow melting.

Figure 8 presents the variations of the erosion rate with the jet velocity and the Reynolds number. For all three regimes, the erosion rate is a strong function of the jet velocity and the Reynolds number. A higher erosion rate is obtained as either the jet velocity or the Reynolds number is increased. For the case without crust formation, transition from laminar to turbulent flow occurs in the Reynolds number range of 5×10^5 to 6×10^5. Upon flow transition, the erosion rate increases at a faster pace with the jet velocity and the Reynolds number. For the case with crust formation, the erosion rates at low Reynolds numbers are more than an order of magnitude lower than those without crust formation whereas the erosion rates at high Reynolds numbers are several times smaller than those with crust formation. However, the rates of erosion for all three melting regimes are at least two to three orders of magnitudes higher than the rates of erosion due to dissolution mass transport. Evidently, when the contact temperature is above the melting point of substrate, the erosion process is dominated by impingement melting heat transport with negligible effects of dissolution mass transport. The latter is important only when the contact temperature is below the substrate melting point.

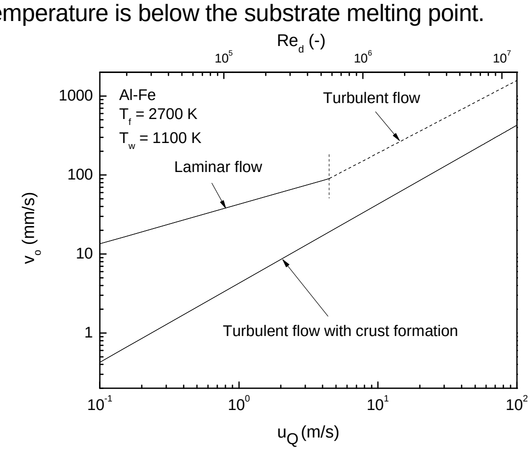

Figure 8. Erosion Rates in the Melting-Controlled Regime

VI. CONCLUSIONS

Based upon the findings of this work, the following conclusions can be made:

- Upon attacked by a solid-propellant fire, erosion of the wall could take place as a result of either melting of the wall or dissolution of the solid substrate into the molten aluminum layer that forms on the wall.
- When the contact temperature at the interface is below the melting point of the wall, erosion of the substrate could take place by dissolution. Under such a situation, the erosion process is dictated mainly by mass transport between the solid substrate and the molten phase.
- For dissolution mass transport, the primary parameters controlling the rate of erosion are the mass diffusivity and the saturated concentration of the aluminum-substrate system. In general, a higher erosion rate is obtained as either the mass diffusivity or the solubility is increased.
- The mass diffusivity and the solubility are strong functions of temperature. Thus the rate of erosion by dissolution mass transport depends strongly upon the temperature at the interface between the solid substrate and the molten layer where erosion takes place. The interface temperature in turn depends on the initial temperatures of the substrate and the molten layer.
- Results of the scaling analysis indicate that the effect of Marangoni flow is negligible compared to the effects of natural convection and/or forced convection. The latter two effects, on the other hand, are equally important and as such, both need to be properly accounted for.
- When subjected to the same temperature and flow conditions, the rate of erosion for the Al-Fe system is always higher than the corresponding rate of erosion for the Al-Ir system. The latter in turn is always higher than the corresponding rate of erosion of the Al-C system.
- When the contact temperature at the interface is above the melting point of the wall, erosion of the substrate would take place due to melting of the wall by the impinging jet. Under such a situation, the erosion process is dictated mainly by impingement melting heat transfer between the solid substrate and the molten phase.
- For impingement melting heat transfer, the primary parameters controlling the rate of erosion are no longer the mass diffusivity and the saturated concentration of the aluminum-substrate system. Rather, the rate of erosion depends primarily on the Stefan number of the system, the jet Reynolds number, and the Prandtl number.
- Three distinctly different regimes of melting have been identified. These are the laminar-flow melting regime, turbulent-flow melting regime without crust formation, and turbulent-flow melting regime with crust formation. The erosion rates are quite different for these three melting regimes. In general, the rate of erosion is highest for turbulent-flow melting regime without crust formation and lowest for the turbulent-flow melting regime with crust formation. The latter could be an order of magnitude lower than the rate of erosion for the laminar-flow melting regime.
- For all three melting regimes, the rates of erosion are at least two to three orders of magnitude higher than the erosion rates due to dissolution mass transport. Thus the erosion process is completely dominated by impingement melting heat transfer once the contact temperature at the interface exceeds the melting point of the substrate. The effects of dissolution mass

transport can be neglected when melting of the substrate occurs.

ACKNOWLEDGMENTS
The work performed at the Pennsylvania State University was supported by the Sandia National Laboratories under Contract No. 826976.

NOMENCLATURE
b thermal property ratio, -
C_s saturated concentration, wt %
c_p specific heat, J/kg-K
D mass diffusion coefficient, m^2/s
d density ratio, -
d_e jet diameter, m
Gr Grashof number, -
g gravitational acceleration, m^2/s
k thermal conductivity, W/m-K
k_B Boltzmann's constant, 1.380 x 10^{-23} J/K
L characteristic length, m
Ma_L Marangoni number, -
Pr Prandtl number, -
R dimensionless ratio defined by equation (9), -
Re Reynolds number, -
r atomic radius in the melt, m
Sc Schmidt number, -
T temperature, K
v_0 rate of erosion, m/s
α thermal diffusivity, m^2/s
β thermal expansion coefficient (volumetric), -
δ thickness of the molten layer, m
$\Delta\rho$ density difference across the molten layer, kg/m^3
ΔT temperature difference across the molten layer, K
μ dynamic viscosity, Pa-s
ν kinematic viscosity, m^2/s
ρ density, kg/m^3
σ surface tension, N/m

Subscripts
c contact
f molten aluminum
i initial contact
l laminar
m molten substance
s solid-liquid interface
t turbulent
w wall (solid substrates)
∞ freestream (ambient)

REFERENCES
Boral, A. A., Cheung, F. B. (2000): "Effects of dissolution on thermosolutal convection in non-isothermal binary metallic systems". *Int. J. Transport Phenomena*, Vol. 2, pp. 187-203.

Boral, A. A., Cheung, F. B., Shiah, S. W. (2002): "Correlations equations for dissolution heat and mass transport in an aluminum-steel system". *Int. J. Transport Phenomena*, Vol. 4, pp. 59-73.

Dybkov, V. I. (1990): "Interaction of 18Cr-10Ni stainless steel with liquid aluminum". *J. Material Sci.*, Vol. 25, pp. 3615-3633.

Epstein, M. (1973): "Heat conduction in the UO2–cladding composite body with simultaneously solidification and melting". *Nucl. Engng. Design*, Vol. 51, pp. 84-87.

Epstein, M., Swedish, M. J., Linehan, J. H., et al. (1980): "Simultaneous melting and freezing in the impingement region of a liquid jet". *AIChE J.*, Vol. 26, pp. 743-749.

Gairola, P. K., Tiwari, R. K., Ghosh, A. (1971): "Rates of dissolution of a vertical nickel cylinder into molten aluminum under free convection". *Metallurgical Trans.*, Vol. 2, pp. 2123-2126.

Guminski, C. (1995), "Diffusion Coefficients in Liquid Metals at High Dilution," in Borgstedt, H. U. and Frees, G. (Eds.), Liquid Metals Systems, Plenum Press, New York.

Hunter, L. W. et al. (2007): "The environment created by an open-air solid rocket propellant fire". *Combustion Sciences Technology*, Vol. 179, pp. 1003-1027.

Iida, T. and Guthrie, R. I. L. (1988), "The Physical Properties of Liquid Metals," Oxford Science Publications, pp. 109-225.

Khina, B. B., Formanek, B., and Solpan, I. (2005): "Limits of applicability of the "diffusion-controlled product growth" kinetic approach to modeling SHS". *Physica B*, Vol. 355, pp. 14-31.

Martin, H. (1977): "Heat and mass transfer between impinging gas jets and solid surfaces". *Advances in Heat Transfer*, Vol. 13, pp.1-60.

Myers, G. E. (1971), "Analytical Methods in Conduction Heat Transfer," McGraw-Hill.

Niinomi, M., Ueda, Y., Sano, M. (1982): "Dissolution of ferrous alloys into molten aluminum". *Trans. Japan Institute of Metals*, Vol. 23, pp. 780-787.

Niinomi, M., Suzuki, Y., Ueda, Y. (1984): "Dissolution of ferrous alloys into molten pure aluminum under forced convection". *Trans. Japan Institute of Metals*, Vol. 23, pp. 780-787.

Nizhenko, V. I. and Floka, L. I. (1972): "Effect of carbon on the surface properties of liquid iron". *Powder Metallurgy and Metal Ceramics*, Vol. 11, pp. 819-823.

Oden, L. L. (1989): "Phase equilibria in the Al-Fe-C system: isothermal sections 1550 ^oC to 2300 ^oC". *Metallurgical Trans. A*, Vol. 20A, pp. 2703-2706.

Predel, B. (1991), "Subvolume a, Ac-Au ... Au-Zr, In O. Madelung (Eds.), Landolt-Bornstein - Group IV: Physical Chemistry, Vol. 5 Phase Equilibria, Crystallographic and Thermodynamic Data of Binary Alloys," pp. 168-189.

Saito, M., Sato, K., Furutani, A., Isozaki, M., Imahori, S., Hattori, Y. (1990): "Melting attack of solid plates by a high temperature liquid jet – effect of crust formation". *Nucl. Eng. Design*, Vol. 121, pp. 11-23.

Saito, M., Sato, K., Furutani, A., Isozaki, M., Imahori, S., Hattori, Y. (1991): "Melting attack of solid plates by a high temperature liquid jet". *Nucl. Eng. Design*, Vol. 132, pp. 171-186.

Shiah, S. W., Yang, B. C., Cheung, F. B., Shih, Y. C. (1998): "Natural convection mass transfer along a dissolution boundary layer in an isothermal binary metallic system". *Int. J. Heat Mass Transfer*, Vol. 41, pp. 3759-3769.